Applied Physics Letters

Radiative thermal conductance between nanostructures

Cite as: Appl. Phys. Lett. **121**, 181105 (2022); https://doi.org/10.1063/5.0108448
Submitted: 08 July 2022 • Accepted: 14 October 2022 • Published Online: 02 November 2022

A. Pérez-Madrid and I. Santamaría-Holek

View Online Export Citation CrossMark

AIP Publishing

© 2022 Author(s).

Applied Physics Letters ARTICLE scitation.org/journal/apl

Radiative thermal conductance between nanostructures

Cite as: Appl. Phys. Lett. **121**, 181105 (2022); doi: 10.1063/5.0108448
Submitted: 8 July 2022 · Accepted: 14 October 2022 ·
Published Online: 2 November 2022

View Online Export Citation CrossMark

A. Pérez-Madrid[1,a)] and I. Santamaría-Holek[2,a)]

AFFILIATIONS

[1]Departament de Física de la Matèria Condensada, Facultat de Física, Universitat de Barcelona, Martí i Franquès 1, 08028 Barcelona, Spain
[2]UMDI-Facultad de Ciencias, Universidad Nacional Autónoma de México Campus Juriquilla, Querétaro 76230, Mexico

Note: This paper is part of the APL Special Collection on Thermal Radiation at the Nanoscale and Applications.
[a)]**Authors to whom correspondence should be addressed:** agustiperezmadrid@ub.edu and isholek.fc@gmail.com

ABSTRACT

Using a properly rescaled Planck's law, the emission spectrum from nanostructures having one or two dimensions in the nanometric length scale is studied. We account for size and shape effects on the radiative heat exchange between nanostructures. This rescaling involves a size-dependent hypothetical temperature obtained from Wien's displacement law. We derive analytical expressions for the absorption cross section and heat conductance in terms of both the length characterizing the shape-anisotropy and the control temperature. Comparison with the experimental data shows a remarkable agreement.

Published under an exclusive license by AIP Publishing. https://doi.org/10.1063/5.0108448

Planck's law describes the radiative heat transfer between macroscopic bodies of any shape and at different temperatures when one considers real body emissivities and geometrical view factors.[1–3] However, recent experiments in the near-field[4–8] have shown that classical Planck's description is valid only when the distances between both bodies are larger than the corresponding thermal photon-length λ_T. When the separation is shorter than λ_T, an increase in the radiative thermal conductance appears overcoming the classical Planck's description.[1,9–11] A similar super-Planckian behavior of the radiative heat conductance is also reported in the far-field regime for two pads having a micrometer-sized area and a nanometer thickness.[12] Analogous effect is observed in the photoluminescence of thin films and in (surface-enhanced Raman scattering).[7,13–16]

The theoretical explanation of the super-Planckian behavior in both the near and far-field regimes has been given along the lines of fluctuational electromagnetism, based on the Maxwell equations and the fluctuation–dissipation theorem.[4] In the far-field, the radiation heat theory has been used to explain the super-Planckian behavior by modifying the photonic density of states of the anisotropic nanostructure.[17]

These experimental and theoretical evidences lead to a crisis in the classical radiative heat transfer theory based on Planck's law, both in the near- and far-field limits already discussed.[9–11,17–19] Nonetheless, it was recently shown that in the near-field regime under a proper rescaling to avoid energy divergences, Planck's law succeeds in describing the phenomenon of spectral thermal emission.[20,21] Here, we show that in the far-field radiative heat exchange between two thin membranes, the super-Planckian behavior can be accounted for by using a properly rescaled Planck's distribution which includes the dependence on the shape-anisotropy parameters. In doing this, we have to consider a phenomenological model for the line shape-function accounting for the temperature and frequency dependence of the absorption cross section.

Our method entails shifting the frequencies to a more energetic region. This accounts for the quantum effects induced by the confinement and allows one to avoid the divergences of the energy spectrum at very short wavelengths.[21] Furthermore, this frequency shifting is concomitant with a rescaling of the temperature in agreement with Wien's law. Consistently, the Planck distribution becomes squeezed.

The Wien's law introduces a length scale that can be correlated with the geometric characteristics of the devices. In this form, in the near-field, this length scale is given by the distance between the emitting bodies, and in the far-field case, this is determined by the physical dimensions of the body itself. Thus, the frequency shifting and the anisotropy-shape of the nanostructures are necessary, but not sufficient, conditions to account for experiments.[12] In addition, one has to take into account the adequate spectral line shape. This line shape depends both on temperature and characteristic length, and it is equivalent to introduce a modified density of states for the emitted radiation.

Published under an exclusive license by AIP Publishing

A size-dependent hypothetical temperature θ emerges from the Wien's displacement law. If λ_θ is the Wien's length at temperature θ, then

$$\frac{\lambda_T}{\lambda_\theta} = \frac{\theta}{T}. \tag{1}$$

The previous relation implies that a rescaling of length brings about a rescaling of temperature. The temperature θ plays the role of a hypothetical temperature which is usually understood as the temperature of a hypothetical black body emitting the same total amount of electromagnetic radiation as the real body.[22]

If ξ is the characteristic length, assuming $\lambda_\theta \sim \xi$, then the hypothetical temperature obeys $\theta\xi \sim T\lambda_T$, where the meaningful situation occurs when $\xi \ll \lambda_T$. Here, temperature rescaling and Wien's law imply a redefinition of the energy domain of the following form:

$$\hat{\nu}\xi = \nu\lambda_T. \tag{2}$$

This scale transformation shifts the frequency domain toward the high-frequency region, maintaining invariant the Bose–Einstein distribution,

$$\hat{N}(\hat{\nu}, \xi) = \frac{1}{\exp\left(\dfrac{h\hat{\nu}}{k_B\theta(\xi)}\right) - 1}. \tag{3}$$

Physically, this scale invariance means that the shape anisotropy controls the frequency through the characteristic nanoscopic length of this anisotropy. This scale transformation also implies that, in thermal equilibrium, the rescaled energy density of electromagnetic radiation of an equivalent hypothetical blackbody (HBB) becomes

$$\hat{u}(\hat{\nu}) = \frac{8\pi\hat{\nu}^2}{c^3}\frac{h\hat{\nu}}{\exp\left(\dfrac{h\hat{\nu}}{k_B\theta}\right) - 1}. \tag{4}$$

Figure 1 shows the effect of the frequency rescaling on the radiated spectral power. For a planar membrane with micrometer area and sub-thermal wavelength thickness ($\xi/\lambda_T \sim 0.027$) at T = 300 K (infrared frequencies-blue dotted line), the maximum of the rescaled distribution takes place in the visible frequency region (green-dashed dotted line) implying a higher hypothetical temperature.

Equation (4) can be written in terms of the control temperature T by introducing a chemical potential[21,23,24]

$$\frac{h\hat{\nu} - \hat{\mu}}{k_B T} = \frac{h\hat{\nu}}{k_B\theta}. \tag{5}$$

From Eqs. (2) and (5), it is possible to write the following relation:

$$h\hat{\nu} - \hat{\mu}(\hat{\nu}) = h\hat{\nu}\frac{\xi}{\lambda_T}. \tag{6}$$

This formula resembles that of the photoelectric effect since the first term at the left-hand side is the incident energy per photon, whereas the second term can be interpreted as the energy necessary for the activation of the surface vibrational and electronic collective modes. Thus, the term at the right-hand side is the remaining energy at disposal for being emitted by the body which, following our previous work,[21] we

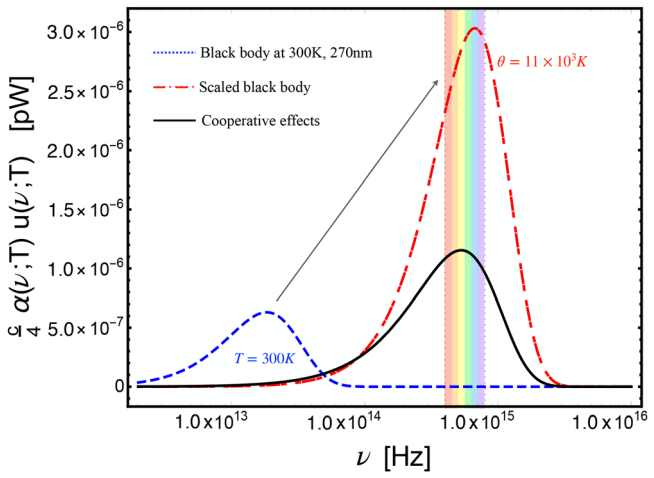

FIG. 1. Spectral power radiated by a pad of dimensions $l_x = 60\,\mu$m, $l_y = 60\,\mu$m, and thickness $\xi = 270$ nm. The dotted blue line is the real blackbody limit (BB) distribution without size correction. The rescaled distribution of the hypothetical blackbody limit (HBB) at a hypothetical temperature θ is represented by the red dashed-dotted line multiplied by 10^{-3}. The black solid line is the fractional approach of the HBB associated with cooperative effects multiplied by 10. Further explanations in the text.

call configuration energy, $E_{con}(\hat{\nu}, \xi) = h\hat{\nu}\xi/\lambda_T$. Since the magnitude of this configuration energy is proportional to the ratio ξ/λ_T, this imposes that the present theory is valid for $\xi/\lambda_T < 1$.

The configuration energy given by the previous equation admits, however, a second interpretation. It is the modified gap energy between the valence and the conduction bands in the material due to quantum confinement effects associated with the nanoscale characteristic length.[21,25] This interpretation is in good agreement with the linear dependence of the energy gap on the control temperature T observed in thin-film photoluminescence experiments.[14]

The energy irradiated $I(\nu)$, per frequency band, by a small body is given by the following relation: $d_\nu I = c\alpha(\nu)u(\nu)d\nu$, where c is the speed of light in vacuum and $\alpha(\nu)$ is the absorption cross section.[26,27] This later quantity becomes modified by the shape and size of the systems.

The differential energy irradiated by a volume V per unit time can be written as

$$d_{\hat{\nu}}\dot{E} = \frac{1}{\tau}VE_{con}(\hat{\nu}, \xi)\hat{N}(\hat{\nu}, \xi)\rho_D(\hat{\nu})d\hat{\nu}, \tag{7}$$

where $\rho_D(\hat{\nu}) = 8\pi\hat{\nu}^2/c^3$ is the Debye density and τ is a frequency-dependent characteristic time. Likewise, Eq. (7) can be rewritten in the following form:

$$d_{\hat{\nu}}\dot{E} = \frac{c}{4}\left[\frac{1}{\tau}\frac{4V}{c}\frac{\xi}{\lambda_T}\right]\hat{u}(\hat{\nu}, \xi)d\hat{\nu}. \tag{8}$$

Comparison of the previous equation with the well-known spectroscopic expression[28] for the absorption cross section allows us to identify

$$\alpha(\hat{\nu}, \xi) = \frac{4}{\tau}\frac{V}{c}\frac{\xi}{\lambda_T}. \tag{9}$$

The previous expressions lead us to write

Published under an exclusive license by AIP Publishing

$$d_{\hat{\nu}}\dot{E} = \frac{c}{4}\alpha(\hat{\nu},\xi)\,\hat{u}(\hat{\nu},\xi)d\hat{\nu}, \tag{10}$$

which is the differential energy irradiated by the body per unit time in terms of the size-dependent absorption cross section.

The energy irradiated per unit time by a small body follows from Eq. (10) by performing an integration over all possible values of the scaled frequency $\hat{\nu}$. Two cases are considered below, reflecting different possibilities for the frequency dependence of the absorption cross section.

In the BB limit, $\xi \sim \lambda_T$ and hence, $\theta \sim T$. In this limit, the characteristic time τ can then be estimated from the wavelength relation $\xi\hat{\nu} = c$ and the Heisenberg's principle $h\hat{\nu}\,\tau \geq h$. It follows that $\tau \sim \xi/c$. Thus, from Eq. (9), we have

$$\alpha_{BB} = 4\frac{V}{\xi} \tag{11}$$

and the expression for the total intensity radiated is

$$I_{BB} = c\frac{V}{\xi}\int_0^\infty u(\nu)d\nu = \frac{V}{\xi}\,\sigma T^4, \tag{12}$$

where σ is the Stefan–Boltzmann constant.

We now apply the previous treatment to cases in which the characteristic time depends on frequency: $\tau(\hat{\nu})$. Molecular spectroscopy[28] shows that the absorption cross section is a function of the frequency that involves the spectral line shape $g(\hat{\nu})$. In view of this, and taking into account Eqs. (9) and (10), we define $\tau^{-1} = \hat{\nu}\,g(\hat{\nu})$. Therefore, the absorption cross section is given by

$$\alpha(\hat{\nu},\xi) = 4\frac{\hat{\nu}}{c}g(\hat{\nu})V\frac{T}{\theta} = 4\frac{\hat{\nu}}{c}g(\hat{\nu})V\frac{\xi}{\lambda_T}. \tag{13}$$

The spectral line shape depends implicitly on a characteristic time needed to deactivate the excited states in the emitting material. This time depends on radiative decays and on processes such as electron collisions or on the interactions between different excited modes (plasmons, polaritons, and excitons).[11,29]

Excitation of different modes and their mutual interaction induces the dependence of the line shape on the temperature. Several mechanisms underlie this dependence.[28] In particular, the case of the Doppler effect introduces a Gaussian distribution of frequencies wider than the natural spectral line shape determined by a Lorentzian formula and associated with purely radiative deactivation processes. Here, we avoid mathematical complications by assuming that the spectral line shape contains the product of two factors

$$g(\hat{\nu}) = f(T)\tilde{g}(\hat{\nu}), \tag{14}$$

where $f(T)$ only depends on the control temperature and can be roughly described by the maximum contribution of the Doppler effect

$$f(T) \sim \left(\frac{m_{eff}c^2}{2k_BT\hat{\nu}_{res}^2}\right)^{1/2}. \tag{15}$$

Here, m_{eff} is an effective mass, and $\hat{\nu}_{res}$ is the resonant frequency.

The spectral line shape $g(\hat{\nu})$ responds to the specific combination of emission sources and deactivation processes within the material. In complex materials or in conditions for which the coupling of different excited modes is strong enough, it is plausible to expect that the frequency dependence of the absorption cross section becomes anomalous, meaning that a series of modes with different relaxation times become coupled. This coupling leads to an anomalous dependence of the spectral line shape on the frequency.

A classical approach to this anomalous behavior is to assume that the spectral line shape takes the form of the imaginary part of the Cole–Cole susceptibility function[28,30]

$$\tilde{g}(\hat{\nu}) = \frac{(\tau_{res}\hat{\nu})^{\delta}\sin(\pi\delta/2)}{1 + 2(\tau_{res}\hat{\nu})^{\delta}\cos(\pi\delta/2) + (\tau_{res}\hat{\nu})^{2\delta}}. \tag{16}$$

Here, δ is the characteristic exponent of the relaxation process and τ_{res} is the time at which the maximum of the absorption function occurs. Additionally, notice that when $\delta < 1$ we have the classical response behavior associated with the Cole–Cole function.[30] However, for $\delta > 1$, the response is associated with an enhanced response.

The fundamental resonance frequency can be assumed as $\tau_{res}^{-1} \simeq k_BT/h$. Then, it is possible to show that, for $\xi/\lambda_T < 1$, the spectral line shape can be expressed in an approximated fractional form by[31]

$$\tilde{g}(\hat{\nu}) \simeq \sin\left(\frac{\pi\delta}{2}\right)\left(\frac{\xi}{\lambda_T}\right)^{\delta}\left(\frac{h\hat{\nu}}{k_BT}\right)^{-\delta}. \tag{17}$$

Therefore, by using Eqs. (14), (15), and (17), in this approximation, the absorption cross section takes the following form:

$$\alpha_\delta \simeq 4\frac{k_BT}{hc}\frac{\phi}{T^{\frac{3}{2}}}\sin\left(\frac{\pi\delta}{2}\right)\left(\frac{\xi}{\lambda_T}\right)^{\delta}V\left(\frac{h\hat{\nu}}{k_BT}\right)^{1-\delta}, \tag{18}$$

where $\phi = [m_{eff}c^2h^2/(2k_B^3)]^{1/2}$ has been introduced to simplify the notation of the formula.

Using the last equation, it is possible to obtain the following relation:

$$\frac{I_\delta(T,\xi)}{\sigma T^4} = B_\delta\frac{k_BT}{hc}\sqrt{\frac{1}{T^3}}\sin\left(\frac{\pi\delta}{2}\right)\left(\frac{\lambda_T}{\xi}\right)^{4-\delta}V, \tag{19}$$

where, for notation simplicity, we have defined the constant B_δ by

$$B_\delta \equiv \frac{60}{\pi^4}\Gamma(5-\delta)\zeta(5-\delta)\phi. \tag{20}$$

Here, $\zeta(x)$ is the Riemman's zeta function.

Verification of the validity of our approach deals with the determination of the heat conductance between two anisotropic bodies at different temperatures, $T_1 < T_2$.

The total energy radiated per unit time is

$$I_{tot}(T,\xi) = I_{BB}(T) + I(T,\xi), \tag{21}$$

where $I_{BB}(T)$ is given by Eq. (12) and $I(T,\xi)$ can be taken from Eqs. (20) and (19). The heat exchanged between two bodies of the same shape is

$$\dot{Q} = F_{1,2}(\xi/d)[I_{tot}(T_2,\xi) - I_{tot}(T_1,\xi)]. \tag{22}$$

Here, $F_{1,2}(\xi/d)$ is the view factor, a quantity that depends on the body separation $d \gg \lambda_T$.[32]

A first order expansion of Eq. (22) in the temperature difference $\Delta T = T_2 - T_1$ yields

Published under an exclusive license by AIP Publishing

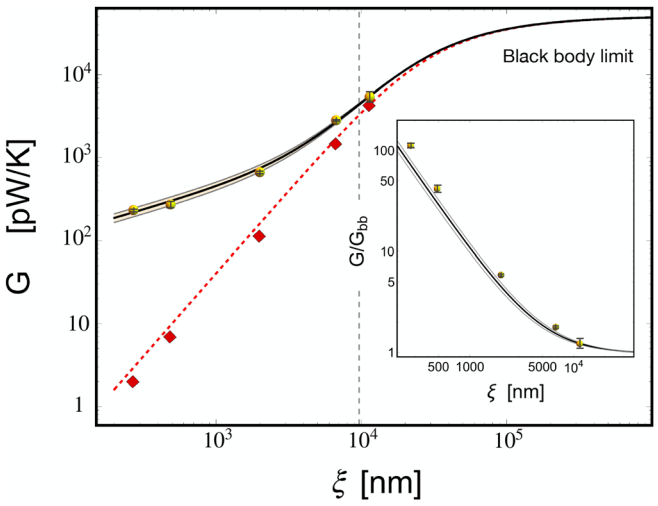

FIG. 2. Heat conductance corresponding to the radiative heat exchange between two pads of dimensions $l_x = 60\,\mu$m, $l_y = 60\,\mu$m, and variable thickness ξ. The red squares (BB) and yellow circles (non-BB) are the experimental results from Ref. 12. The solid black line comes from Eq. (24). The dotted red line corresponds to Eq. (25). The fits were performed using T = 300 K, $\lambda_T = 9.8\,\mu$m, $D = 0.133$ nm, $\delta = 1.5$, and $m_{eff} = 3.63 \times 10^{-12}$ kg (black line). The upper gray line corresponds to $m_{eff} = 4.76 \times 10^{-12}$ kg, whereas the lower gray line corresponds to $m_{eff} = 2.80 \times 10^{-12}$ kg. The inset shows the ratio G_δ/G_{bb}. Details in the text.

$$\dot{Q}_\xi = -G(\xi)\Delta T, \tag{23}$$

where $T = (T_1 + T_2)/2$ is the average temperature and $G(\xi)$ is the heat conductance.

Cooperative effects lead to

$$G_\delta = 4F_{1,2}\frac{V}{\xi}\left[1 + \sin\left(\frac{\pi\delta}{2}\right)\frac{k_B B_\delta}{hc}\frac{1}{T^{\frac{1}{2}}}\frac{(\lambda_T)^{4-\delta}}{\xi^{3-\delta}}\right]\sigma T^3. \tag{24}$$

Notice that Eq. (24) introduces two parameters, the exponent δ and the effective mass m_{eff}, associated with the emergence of strongly coupled excited modes. Both quantities imply non-trivial relations for the density of states of several coupled optical and thermal modes in the material.[11]

Figure 2 shows the heat conductance in terms of the thickness of two parallel pads with variable thickness ξ. The red squares are BB simulations from the far-field radiation theory, and the yellow circles are the non-BB data both reported in Ref. 12. The ideal BB heat conductance (red line) scales with the thickness according to the view factor $F_{1,2}$. The solid black line represents the fit using Eq. (24) with an emission volume given by $V = w\,D\,\xi$. Since the width is $w = l_x = 60$ nm, we obtain that the depth is given by $D = 0.133$ nm. This fact means that the radiation is emitted by a thin sheet of atoms at the surface. Let us notice that the ideal BB heat-conductance without size effects is given by

$$G_{bb} = 4F_{1,2}\sigma T^3, \tag{25}$$

which needs to be multiplied by the factor V/ξ in order to reproduce the data computed using the far-field radiation theory with emissivity of 1 (red squares). The gray dashed line indicates the position of the Wien's length at T = 300 K.

The BB heat conductance (red squares and lines) inherits the scaling of the view factor F_{12} between two square surfaces of size ξ.[32,33] For $\xi \gg \lambda_T$, the curve exhibits a constant plateau (gray dashed line). The theoretical expression incorporating the shape of the body, Eq. (24), also shows this saturation behavior. However, for $\xi < \lambda_T$, the heat conductance separates from the BB behavior, indicating that the contribution of the absorption cross section becomes increasingly important. The experimental data (yellow circles) and the fractional approach (24) indicate that the heat conductance follows a power-law behavior for $\xi < \lambda_T$. This scaling and the value of the effective mass (if the Doppler mechanism is interpreted in terms of a single charge carrier contribution), suggests the cooperation of different absorption mechanisms dependent on the system's size. The exponent used to fit the data is larger than the unit suggesting an enhancement of the

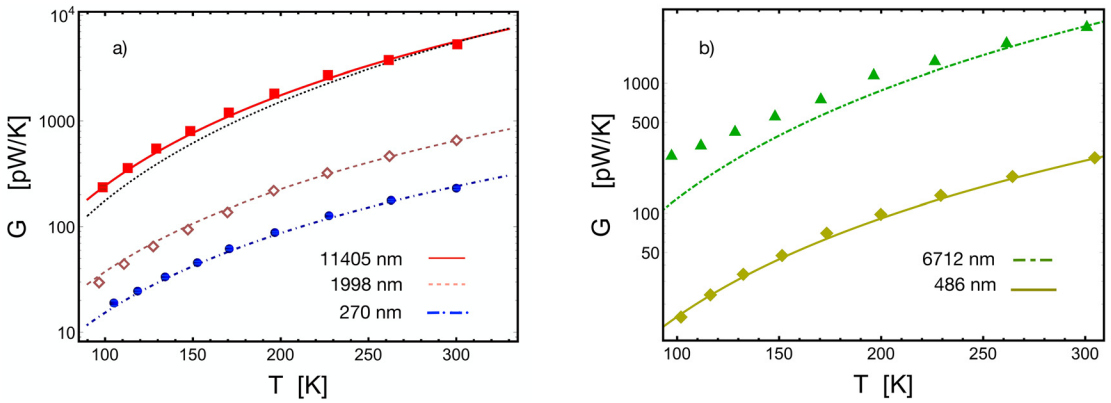

FIG. 3. Heat conductance as a function of the temperature for different thicknesses. The symbols are the experimental data taken from Ref. 12 and the lines correspond to Eq. (24). (a) Data for $\xi = 270$ (blue), 1998 (pink), and 11 405 (red). (b) Data for $\xi = 486$ (dark yellow) and 6712 (green). The dotted black line in (a) for 11 405 nm has been generated by neglecting the temperature dependence of the line shape function. The fits were performed using $D = 0.133$ nm and $\delta = 1.5$ in all cases. For $\xi = 270$ and 11 405 nm, we used $m_{eff} = 4.76 \times 10^{-12}$ kg (relative error in 5%–10%). For $\xi = 486$ and $\xi = 1998$ nm, we used $m_{eff} = 2.8 \times 10^{-12}$ kg (relative error of 8%–10%). For $\xi = 6712$ nm, we used $m_{eff} = 4.76 \times 10^{-12}$ kg (relative error of 50%).

Published under an exclusive license by AIP Publishing

interactions between different modes associated with the absorption-emission process.[28]

The temperature dependence of the heat conductance seems to support the above-mentioned conclusions on enhanced mode interactions [see Figs. 3(a) and 3(b)]. Using a phenomenological model for the line shape broadening of the type observed in the Doppler effect, with the characteristic frequency given by $\hat{\nu}_{res} = k_B T/h$, provides a very good correspondence between experiment[12] (symbols) and theory [Eq. (24)] for different fixed thicknesses. Neglecting the temperature dependence of the line shape does not allow the reproduction of the temperature trend of the heat conductance [see the dotted black line in Fig. 3(a)]. This second case shows heat conductance trends in the temperature that are very similar to those found by the FFRHT (far-field radiative heat transfer).[12] The complete approach given by Eq. (24) has a very similar behavior as the FED (fluctuation electrodynamics) simulations.[12]

To finish, since the absorption coefficient γ, proportional to the absorption cross section, can be obtained in terms of the correlation between the dipolar moments of the system through the Fourier transform,[34,35]

$$\gamma(\hat{\nu}, \xi) = \frac{1}{2\pi} \int e^{i\omega t} \langle \mu(0)\mu(t) \rangle dt, \tag{26}$$

where $\omega = \hat{\nu}/2\pi$ and the brackets $\langle \mu(0)\mu(t) \rangle$ indicate the equilibrium statistical average, we can establish an expression (26) of the fluctuation–dissipation theorem for the dipolar moments in a nanometric anisotropic body.[35,36]

The strong confinement by the asymmetry enhances couplings among active modes leading to an anomalous dependence of the absorption coefficient in terms of the frequency, characterized by the exponent δ. This coupling yields a power-law function of relaxation times of the dipoles' orientations. This later effect together with the hypothetical temperature suggests that dipolar-moment fluctuations may follow a modified form of the fluctuation–dissipation theorem.

A. Pérez-Madrid is grateful to the Ministerio de Ciencia e Innovación (MCNN) (Project Reference No. PID2021-126570NB-I00). I.S.H. acknowledges UMDI-J for the financial support by internal grant with No. 115377. Both authors acknowledge Dr. Saúl I. Hernández for useful discussions on the properties of the anomalous dielectric constant.

AUTHOR DECLARATIONS

Conflict of Interest

The authors have no conflicts to disclose.

Author Contributions

Agustin Perez-Madrid: Conceptualization (equal); Formal analysis (equal); Investigation (equal); Writing – original draft (equal); Writing – review & editing (equal). **Ivan Santamaría-Holek:** Conceptualization (equal); Formal analysis (equal); Writing – original draft (equal); Writing – review & editing (equal).

DATA AVAILABILITY

The data that support the findings of this study are available from the corresponding authors upon reasonable request.

REFERENCES

[1]J. C. Cuevas and F. J. Garcia-Vidal, "Radiative heat transfer," ACS Photonics **5**, 3896 (2018).
[2]R. Incardone, T. Emig, and M. Kruger, "Heat transfer between anisotropic nanoparticles: Enhancement and switching," Eur. Phys. Lett. **106**, 41001 (2014).
[3]M. L. E. Rousseau and J. J. Greffet, "Asymptotic expressions describing radiative heat transfer between polar materials from the far-field regime to the nanoscale regime," Appl. Phys. **111**, 014311 (2012).
[4]A. I. Volokitin and B. N. Persson, "Near-field radiative heat transfer and noncontact friction," Rev. Mod. Phys. **79**, 1291 (2007).
[5]J. Mulet, K. Joulain, R. Carminati *et al.*, "Enhanced radiative heat transfer at nanometric distances," Microscale Thermophys. Eng. **6**, 209 (2002).
[6]S. Biehs, E. Rouseau, and J. Greffet, "Mesoscopic description of radiative heat transfer at the nanoscale," Phys. Rev. Lett. **105**, 234301 (2010).
[7]M. Kruger, T. Emig, and M. Kardar, "Nonequilibrium electromagnetic fluctuations: Heat transfer and interactions," Phys. Rev. Lett. **106**, 210404 (2011).
[8]R. Messina and M. Antezza, "Casimir-Lifshitz force our of thermal equilibrium and heat transfer between arbitrary bodies," Eur. Phys. Lett. **95**, 61002 (2011).
[9]P. O. Chapuis, S. Volz, C. Henkel *et al.*, "Effects of spatial dispersion in near-field radiative heat transfer between two parallel metallic surfaces," Phys. Rev. B **77**, 035431 (2008).
[10]C. Lucchesi, R. Vaillon, and P.-O. Chapuis, "Radiative heat transfer at the nanoscale: Experimental trends and challenges," Nanoscale Horiz. **6**, 201–208 (2021).
[11]K. Joulain, R. Carminati, J.-P. Mulet *et al.*, "Definition and measurement of the local density of electromagnetic states close to an interface," Phys. Rev. B **68**, 245405 (2003).
[12]D. Thompson, L. Zhu, R. Mittapally *et al.*, "Hundred-fold enhancement in far-field radiative heat transfer over the blackbody limit," Nature **561**, 216 (2018).
[13]S. Cho, J. Ma, Y. Kim *et al.*, "Photoluminescence and ultraviolet lasing of polycrystalline ZnO thin films prepared by the oxidation of the metallic Zn," Appl. Phys. Lett. **75**, 2761 (1999).
[14]C. Chen, F. Chen, X. Chen *et al.*, "Bright mid-infrared photoluminescence from thin-film black phosphorus," Nano Lett. **19**, 1488–1493 (2019).
[15]M. J. Mulvihill, X. Y. Ling, J. Henzie *et al.*, "Anisotropic etching of silver nanoparticles for plasmonic structures capable of single-particle SERS," J. Am. Chem. Soc. **132**, 268–274 (2010).
[16]A. I. Pérez-Jiménez, D. Lyu, Z. Lu *et al.*, "Surface-enhanced Raman spectroscopy: Benefits, trade-offs and future developments," Chem. Sci. **11**, 4563 (2020).
[17]J. Cuevas, "Thermal radiation from subwavelength objects and the violation of Planck's law," Nat. Commun. **10**, 3342 (2019).
[18]R. C. Hilborn, "Einstein coefficients, cross sections, *f* values, dipole moments, and all that," Am. J. Phys. **50**, 982 (1982).
[19]A. Narayanaswamy, S. Shen, L. Hu *et al.*, "Breakdown of the Planck blackbody radiation law at nanoscale gaps," Appl. Phys. A **96**, 357 (2009).
[20]T. P. Weldon, "Rayleigh and Mie enhancement of blackbody radiation in nanoscale devices," in *IEEE Southeastcon 2009* (IEEE, 2009), pp. 216–220.
[21]I. Santamaría-Holek and A. Pérez-Madrid, "Scaling Planck's law: A unified approach to the Casimir effect and radiative heat-conductance in nanogaps," Nanoscale Horiz. **7**, 526 (2022).
[22]L. Landau and E. Lifshitz, *Statistical Physics* (Pergamon Press, Oxford, 1989).
[23]P. Wurfel, "The chemical potential of radiation," J. Phys. C **15**, 3967 (1982).
[24]H. Ries and A. McEvoy, "Chemical potential and temperature of light," J. Photochem. Photobiol. A **59**, 11 (1991).
[25]I. Santamaria-Holek, J. Lopez-Alamilla, and A. Perez-Madrid, "Power conversion efficiency of non-equilibrium light absorption," AIP Adv. **7**, 045004 (2017).
[26]L. Landau, E. Lifshitz, and L. Pitaevskii, *Electrodynamics of Continuous Media* (Elsevier, Amsterdam, 2008).
[27]O. Stenzel, *Light-Matter Interaction* (Springer, Cham, Switzerland, 2022).
[28]J. L. McHale, *Molecular Spectroscopy* (CRC Press, Boca Raton, FL, 2017).

Published under an exclusive license by AIP Publishing

[29]K. Joulain, J.-P. Mulet, F. Marquier *et al.*, "Surface electromagnetic waves thermally excited: Radiative heat transfer, coherence properties and Casimir forces revisited in the near field," Surf. Sci. Rep. **57**, 59–112 (2005).
[30]K. S. Cole and R. H. Cole, "Dispersion and absorption in dielectrics I. Alternating current characteristics," J. Chem. Phys. **9**, 341 (1941).
[31]S. S. Nekrashevich and V. A. Gritsenko, "Electronic structure of silicon dioxide (a review)," Phys. Solid State **56**, 207–222 (2014).
[32]T. L. Bergman and A. S. Lavine, *Fundamentals of Heat and Mass Transfer* (Wiley, New York, 2017).
[33]V. Fernández-Hurtado, A. Fernández-Domínguez, J. Feist *et al.*, "Super-Planckian far-field radiative heat transfer," Phys. Rev. B **97**, 045408 (2018).
[34]R. Kubo, "The fluctuation-dissipation theorem," Rep. Prog. Phys. **29**, 255 (1966).
[35]R. Zwanzig, *Nonequilibrium Statistical Mechanics* (Oxford University Press, New York, 2001).
[36]I. Santamaria-Holek and A. Perez-Madrid, "Eyring equation and fluctuation-dissipation far away from equilibrium," J. Chem. Phys. **153**, 244116 (2020).

Published under an exclusive license by AIP Publishing